Seismically determined elastic parameters for Earth's outer core: Supplementary material

Jessica C.E. Irving,[1*] Sanne Cottaar,[2] Vedran Lekić[3]

[1]Dept. of Geosciences, Princeton University, NJ, USA,
[2]Dept. of Earth Sciences, University of Cambridge, UK
[3]Dept. of Geology, University of Maryland, College Park, MD, USA
*To whom correspondence should be addressed; E-mail: jirving@princeton.edu.

This supplementary material presents details of the Birch-Murnaghan (BM) parameterization and resulting EPOC-BM model (Sections 1 and 2) and details of inversions using a dataset from the PREM study (Section 3) and with STW105 as a base model (Section 4). More background to the EPOC model is given including the prior tests used in the inversion (Section 5), differential travel time calculations for a number of core-sensitive phases allowing the comparison of EPOC to other 1D models (Section 6), and information about the non-linear dependence of the mode center frequencies on the elastic parameters (Section 7). Also presented for reference are the center frequencies and uncertainties of the mode dataset used in the study (Section 8), the outer core velocity and density as a function of depth for the EPOC-Vinet and EPOC-BM models (Section 9).

1 Birch-Murnaghan equation-of-state

The Birch-Murnaghan equation-of-state, to the third order, along an isentrope is used to parameterize the outer core density and velocity and is expressed in the same three parameters as the Vinet EoS: K_{0S}, the bulk modulus at ambient conditions, K'_{0S} the derivative of the bulk modulus with pressure, and V_0 the molar volume at ambient conditions. All of these parameters are taken to be at constant entropy. The Birch-Murnaghan EoS formulation (as implemented in BurnMan (*30, 32*)) is solved to retrieve molar volume, V, at pressure, P:

$$P = 3K_{0S} f \left(1 + 2f\right)^{5/2} \left[1 + \frac{3}{2}\left(K'_{0S} - 4\right) f\right], \tag{1}$$

with

$$f = \frac{1}{2}\left[\left(\frac{V}{V_0}\right)^{-2/3} - 1\right]. \tag{2}$$

Similar to the procedure for the Vinet EoS, we use a fixed molar mass M of 0.05 kg/mol to and present results for reference density, ρ_0. This is to avoid the inherent trade-offs between molar mass and molar volume. Starting with PREM pressures, the densities and resulting pressures are again iterated until convergence.

The Birch-Murnaghan formulation further defines the isentropic bulk modulus, K_S:

$$K_S = (1 + 2f)^{5/2}\left[K_{0S} + (3K_{0S}K'_{0S} - 5K_{0S})f + \frac{27}{2}(K_{0S}K'_{0S} - 4K_{0S})f^2\right]. \tag{3}$$

with which we can compute the bulk sound (outer core P-wave) velocity.

2 EPOC-Birch Murnaghan results

Here we present the mineral physics parameters and figures for the EPOC-Birch Murnaghan model. The velocity and density of the EPOC-BM model are very close to those of EPOC-Vinet, but the different formulation of the BM EoS means that the values at ambient conditions are markedly different. This is evidenced by the differences between the EoS parameters which fit PREM best for the two different formulations. For example, PREM's reference isentropic bulk modulus, K_{0S}, is 79.7GPa using the Vinet EoS and 134 GPa using the BM EoS. It is therefore extremely important to use the appropriate EoS when using a particular set of EoS parameters. Doing so leads to the very similar velocity and density models for the outer core shown in tables S3 and S4.

	EPOC-BM	PREM-BM
K_{0S} (GPa) Reference isentropic bulk modulus	120 (113 – 126)	134
K'_{0S} Pressure derivative of K_{0S}	4.60 (4.55 – 4.66)	4.46
ρ_0 (kg/m^3) Reference molar density	6550 (6470 – 6620)	6600
V_0 (m^{-3}) Reference molar volume	7.63×10^{-6} (7.55×10^{-6} – 7.72×10^{-6})	7.57×10^{-6}

Table S1: Elastic parameters for the outer core for the Birch-Murnaghan EoS, and for Birch-Murnaghan EoS fits to PREM. Molar density parameters are given for a fixed molar mass of 0.05 kg. The values in brackets encompass two thirds of the parameter ranges, similar to the 1σ range for normally distributed parameters.

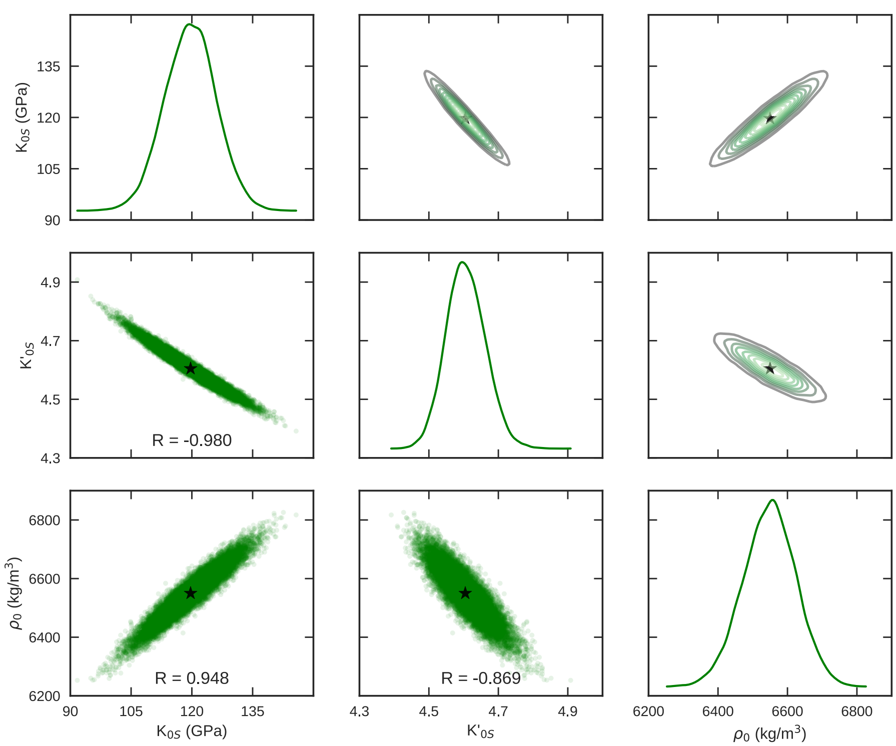

Figure S1: Parameter posterior distributions and trade-offs, for the three Birch Murnaghan EoS parameters. ρ_0 is presented using the fixed molar mass of 0.05 kg and inverted molar volume. The black stars show the median values, used to find the velocity and density models used for the EPOC-BM model in Figure S2.

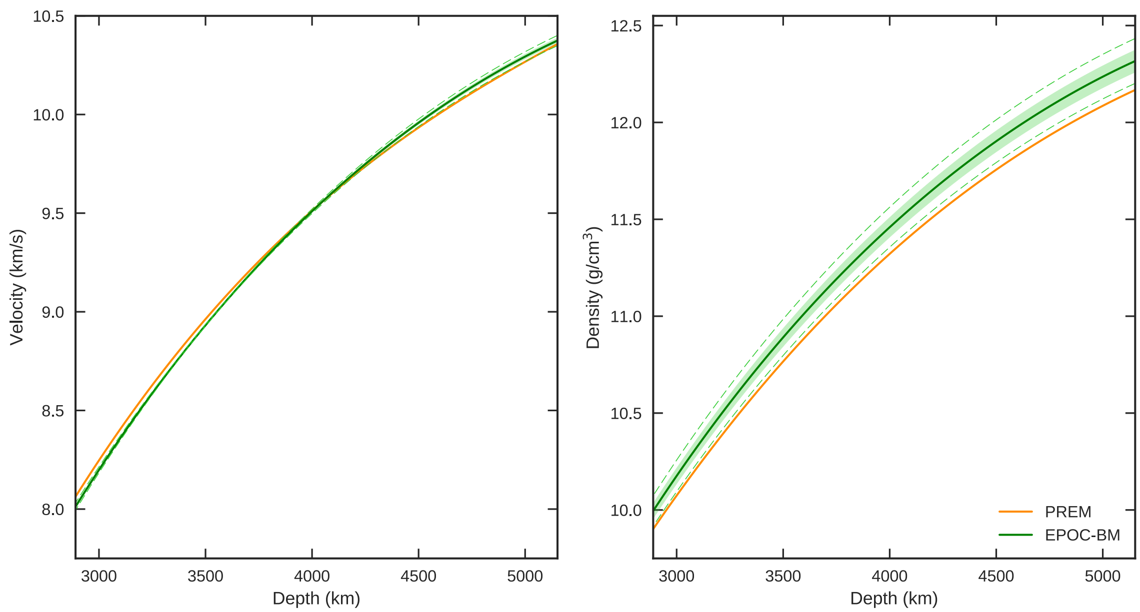

Figure S2: a) P-wave or bulk sound velocities and b) densities for the EPOC-BM models compared to PREM (orange lines). The models produced by the median parameters are shown as the dark green lines, the shaded region encompasses two thirds of the models and the dashed lines contain 95% of the models.

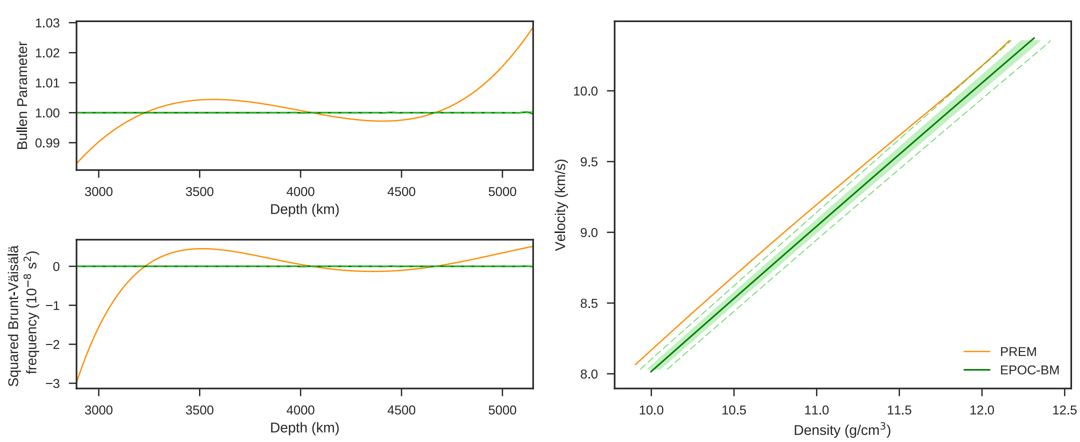

Figure S3: Relevant physical properties of the EPOC-BM model, with PREM shown for comparison: a) Bullen Parameter and b) squared Brunt-Väisälä frequency as a function of depth; c) Velocity as a function of density - linear behavior is required for models to follow Birch's law. Colours as Figure S2.

3 Inversion using PREM data

Our inversion uses an updated data compilation as well as a different parameterization and inversion procedure compared to the study producing PREM (*6*). To understand better which of these changes are responsible for differences between EPOC and PREM, we have carried out an inversion using only the modes also used in the construction of PREM. Specifically, we have used the center frequencies from the PREM paper of the 240 modes in our dataset which were also present in the original PREM inversion, avoiding, for example, inner core sensitive modes. We use the errors as assigned in this study. The results of this inversion are shown in Figure S4. We note that body wave data (SKS, PKP, PKIKP and PcP-PKiKP) were also used in the construction of PREM, while in this test, we only consider the modes common to the two inversions.

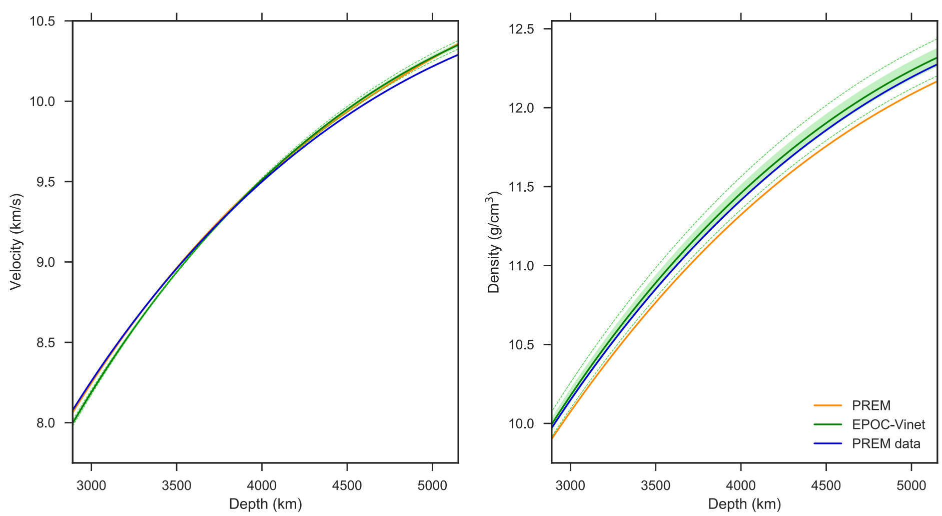

Figure S4: a) P-wave or bulk sound velocities, and b) densities for EPOC-Vinet (green) compared to PREM (orange lines) and the results of the inversion using data from the PREM study (blue). The models produced by the median parameters for EPOC-Vinet are shown as the dark green lines, the shaded region encompasses two-thirds of the values and the dashed lines 95% of the values at each depth

The results of this test show that both the new data and the inversion method are important in allowing us to create our new model of outer core structure. Using the old mode measurements leads to a model with a velocity which is very close to that of PREM in the upper outer core – indeed the lines representing PREM and our inversion using PREM data are not easy to tell apart. The velocity difference at the CMB is 0.0145km/s. Thus, we conclude that our new data set, which consists of updated mode measurements from more recent observational studies (*22–26*) and contains modes not measured for the PREM study, is the reason that EPOC-Vinet has a lower velocity than PREM at the CMB.

The shape of the velocity curve deeper in the outer core, and the density model across the entire outer core are not the same as either PREM or EPOC-Vinet. The velocity in the deeper outer core in our modeling approach is less controlled by the normal mode data set, as inner core sensitive modes are excluded, and the resulting data set has less sensitivity to the deeper outer core (see Figure 5 in the main paper). Velocities at deeper depths are more controlled by the equation of state and therefore by the extrapolation from the constrained velocity gradients at the top of the outer core. The density of this test inversion lies between that of PREM and the EPOC-Vinet model, and at the lower end of the EPOC-Vinet 66% percentile bounds. This illustrates the higher density we find in EPOC-Vinet is not entirely due to the data we use, but could be do to different inversion and parameterization choices between the studies. In the PREM study, density is initially set to fit the Adams-Williamson equation and mass and moment of inertia are included as a constraint in the inversion; either of these might have impacted the final model.

4 Inversion using STW105 for the rest of the Earth

Our inversion is for properties within the outer core; therefore, we assume a fixed model in the mantle and inner core. We partly accommodate this by assigning large error bars to mode center frequencies that are more sensitive to a different model at shallower depths. To further understand the effect of changing the reference model used for the rest of the Earth we carried out a test inversion using STW105 (*28*) to represent the structure of the rest of the Earth. STW105 provides both velocity and density profiles. We use the same modes as in the main paper, and seek the Vinet EoS coefficients and corresponding velocity and density models which best fit the data. The results are shown in Figure S5.

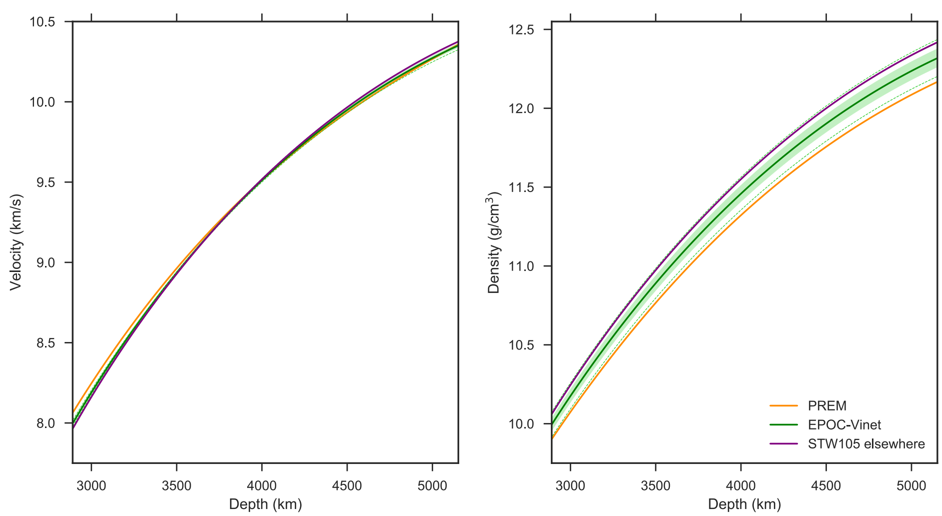

Figure S5: a) P-wave or bulk sound velocities, and b) densities for EPOC-Vinet (green) compared to PREM (orange lines) and the results of the inversion using STW105 to represent structure elsewhere in the Earth (purple). The models produced by the median parameters for EPOC-Vinet are shown as the dark green lines, the shaded region encompasses two-thirds of the values and the dashed lines 95% of the values at each depth.

The outer core velocity obtained assuming STW105 outside the outer core differs from that in EPOC by up to 0.033 km/s. The difference is greatest at the CMB, where this model slower than EPOC-Vinet, which is in turn slower than PREM. Near the inner core, this model is faster than both EPOC-Vinet and PREM. In other words, the model's velocity gradient across the outer core is steeper than that in EPOC-Vinet and PREM. The 95% intervals for the EPOC-Vinet and the STW105-based velocity models overlap everywhere except at depths 323-576 km below the CMB; in this region the width of the interval is narrow (0.009 – 0.018 km/s). When STW105 is assumed outside the outer core, the densities obtained are higher than those in EPOC-Vinet throughout, by 0.066–0.100g/cm^3 from the CMB to ICB respectively. The reduced chi-square misfit is greater for this model than for EPOC-Vinet by 6%. We therefore prefer EPOC-Vinet to this model.

The large error bars on density for EPOC, together with changes in density profiles resulting from changing assumptions about structure outside the outer core, show that density is poorly constrained by mode center frequencies, and sensitive to changes in the mantle. Our results call for the density to be re-evaluated on a global scale. This is beyond the scope of this study, as the parameterization applied here is only a valid assumption for the well-mixed homogeneous outer core. Nevertheless, the fact that densities obtained assuming STW105 outside the outer core are even greater than those of EPOC, and the velocities at the top of the outer core even lower, gives us confidence that the main conclusions of our study, and the distinctive features of EPOC, appear to be robust with respect to an alternative realistic mantle model.

5 Prior geophysical tests

To speed up the Monte Carlo search through the parameter space, we conduct a number of computational inexpensive tests that reject nonphysical models before computing their normal mode eigenfrequencies. Care is taken to ensure that our posterior distribution is not influenced by these prior tests. Firstly, we require that the outer core's mass and MoI must be within 5% of the PREM values. For our final ensemble of models, all of the masses and moments of inertia are are within 3% of PREM, showing that these tests do not affect our parameter distributions. Secondly, we make restrictions on the velocity and density jumps at the CMB and ICB: the outer core's density should be less than that of the inner core; the velocity at the CMB should higher than the shear wave velocity of the mantle; and the velocity at the ICB should be lower than the compressional wave velocity in the inner core. Additionally, models which fail to compute the presence of at least one of the modes observed in the target frequency window of 0.1 – 10 mHz are penalized; all of the accepted models produce all of the modes observed.

6 Body wave differential travel time predictions

Here we show the differential travel time predictions, calculated using the TauP toolkit (*69*) for a range of body wave phase pairs relative to PREM: SKKS-SKS, SKKS-SKKKS, SKKS-SKKKKS, SKKKS-SKKKKS and PKIKP-PKP. Of these phases, the SmKS pairs are sensitive to the top of the outer core, while the PKIKP-PKP pair is sensitive to the lower half of the outer core. The relative differential travel time, $rdt_{ph1-ph2}$, for a pair of seismic phases, $ph1$ and $ph2$, are calculated for a given model, $model$, in reference to PREM as follows:

$$rdt_{ph1-ph2} = \left(t_{ph2}^{model} - t_{ph1}^{model}\right) - \left(t_{ph2}^{PREM} - t_{ph1}^{PREM}\right) \tag{4}$$

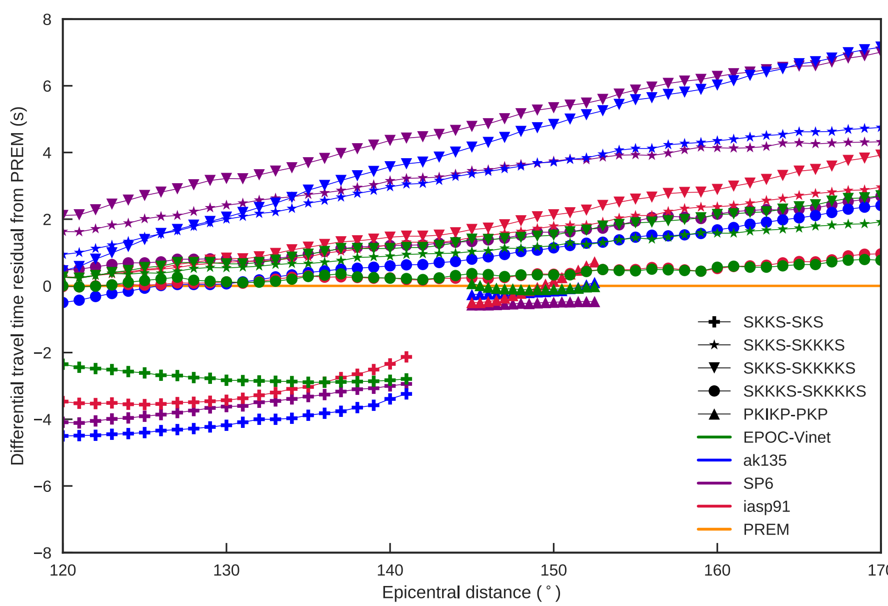

Figure S6: Differential travel time predictions for EPOC-Vinet, ak135, iasp91 and SP6 with respect to predictions for PREM. An event depth of 30km is used.

The predictions of EPOC-Vinet are, for the most part, between those of PREM and the body wave-derived models. We are only able to calculate these relative differential travel times where both elements of the phase pair exist for both PREM and the model in question; thus we do not specifically address here the ranges over which ray theory can predict the presence of certain body wave phases. Beyond the comparison to the observations from (*19*) in the main text, these results provide another independent body wave validation of our velocity profile.

7 Non-linearity of center frequencies

In a non-rotating, spherically-symmetric model of the Earth, the center frequencies of normal modes can be computed by integrating a set of differential governing equations, e.g. (*37*). To first order, Coriolis terms do not affect normal mode center frequencies (*27, 70*). We compute the effects of ellipticity to first order (*27*), and correct our dataset accordingly, though the corrections are nearly negligible. The relationship between perturbations to the elastic properties of the spherically-symmetric Earth and the resulting perturbation to the center frequencies of normal modes is usually linearized using first order perturbation theory. Indeed, to first order, perturbations to the depth-profiles of elastic parameters can be treated in the self-coupling framework (*27*). Because the inaccuracy of this linearization can be greater than the uncertainty of the mode center frequencies (order 10^{-3} for many modes used in this work), its use amounts to a degradation of the measurement precision – and thereby the information content of the dataset, e.g. (*16*). For each mode in our dataset, we compute the center frequency shift due to a 1% change in average v_p in the outer core and compare it to the frequency shift predicted by first order perturbation theory. The absolute difference between the two shifts ($\Delta\omega_{NL}$) is then compared to the to the measurement uncertainty, which accounts for uncertainties due to mantle structure as described in the main text. Figure 7 shows this comparison, with the size of the symbol proportional to the mode's sensitivity to outer core structure. From this figure, we conclude that even a 1% change in outer core properties can yield non-linear effects comparable to (and for some modes, twice as large as) the observational uncertainty. Therefore, in this study, we treat the relationship between mode center frequencies and elastic parameters of the outer core in a fully non-linear fashion, predicting mode frequencies for each proposed model using Mineos.

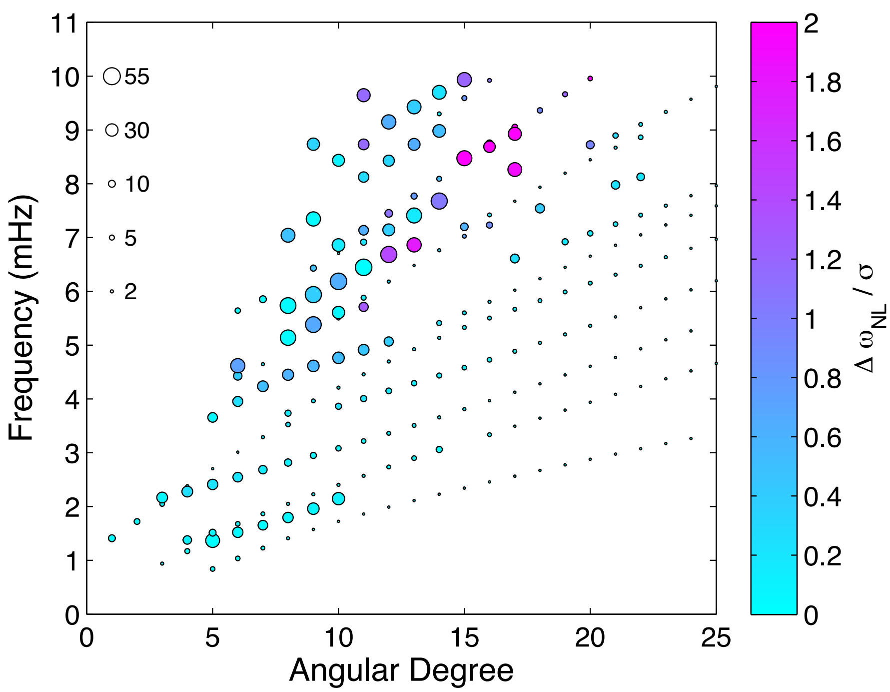

Figure S7: Non-linearity of the relationship between mode center frequency and elastic parameters of the core. Each symbol corresponds to a different mode in our dataset, and its size is proportional to the mode's sensitivity to outer core structure (in percent, see legend in upper left). Symbol color represents the magnitude of the non-linearity of mode frequency shift due to a 1% perturbation to outer core v_p, compared to measurement uncertainty. NB: measurement uncertainty has been adjusted to account for uncertainties in mantle structure, so this figure shows the lower bound on the magnitude of non-linearity for most modes.

8 Mode dataset

Table 2 presents our center frequency dataset.

Table S2: Radial order (n), angular order (l), center frequency, and 1σ uncertainty (see text). Note that, in order to be conservative in our assessment of effect of unmodelled mantle structure, uncertainties below 3.23 μHz are increased to 3.23 μHz in our inversions. The mode frequencies are taken from references (*22–26*) and have been corrected for ellipticity.

n	l	Center frequency (μ Hz)	1σ (μ Hz)	n	l	Center frequency (μ Hz)	1σ (μ Hz).
0	5	840.03	0.089	5	17	5668.76	2.319
0	6	1037.56	0.057	5	18	5829.2	2.733
0	7	1230.98	0.04	5	19	5988.49	3.203
0	8	1412.79	0.196	5	20	6152.22	3.755
0	9	1577.53	0.345	5	21	6310.38	4.405
0	10	1725.61	0.415	5	22	6473.56	5.154
0	11	1861.85	0.389	5	23	6635.42	6.002
0	12	1989.68	0.284	5	24	6800.77	6.938
0	13	2111.97	0.121	5	25	6965.93	7.942
0	14	2230.42	0.08	5	26	7132.65	8.987
0	15	2345.41	0.299	5	27	7291.92	10.035
0	16	2457.46	0.523	5	28	7455.35	11.039
0	17	2566.49	0.733	5	29	7616.87	11.948
0	18	2672.42	0.915	5	30	7778.51	12.708
0	19	2776.82	1.058	5	31	7941.77	13.271
0	20	2878.33	1.155	5	32	8099.05	13.595
0	21	2977.45	1.2	5	33	8253.58	13.653
0	22	3074.57	1.192	5	34	8408.99	13.436
0	23	3170.62	1.133	5	35	8570.58	12.945
0	24	3265.58	1.025	5	36	8726.94	12.201
1	3	940.05	0.615	5	37	8884.49	11.232
1	4	1173	0.89	5	38	9043.66	10.079
1	5	1370.22	1.191	5	39	9200.62	8.789
1	6	1521.59	1.192	5	40	9360.48	7.406
1	7	1654.66	1.125	5	41	9509.99	5.981
1	8	1797.95	1.207	5	42	9679.31	4.559
1	9	1962.04	1.372	5	43	9835.76	3.179
1	10	2146.4	1.533	6	9	3965.01	0.335
1	16	3337.68	0.809	6	10	4211.05	0.567
1	17	3493.48	1.553	6	14	5411.01	0.026
1	18	3643.83	2.118	6	15	5601.25	0.688
1	19	3792.31	2.629	6	16	5806.77	1.34
1	20	3940.04	3.107	6	17	6020.74	1.834
1	21	4085.71	3.553	6	18	6235.7	2.143

Continued on next page.

Table S2 – *Continued from previous page.*

n	l	Center frequency (μ Hz)	1σ (μ Hz)	n	l	Center frequency (μ Hz)	1σ (μ Hz)
1	22	4231.53	3.96	6	19	6446.19	2.225
1	23	4376.3	4.32	6	20	6653.93	2.012
1	24	4521.08	4.628	6	21	6855.24	1.45
1	25	4662.69	4.879	6	22	7050.35	0.545
1	26	4809.15	5.068	6	23	7234.78	0.587
1	27	4952.81	5.194	6	24	7412.52	1.754
1	28	5088.68	5.256	6	25	7588.15	2.763
1	29	5233.05	5.254	6	26	7756.15	3.489
1	30	5373.08	5.189	6	27	7921.95	3.881
1	31	5513.56	5.066	6	28	8088.19	3.948
1	32	5652.38	4.885	6	29	8255.79	3.728
1	33	5788.83	4.653	6	30	8417.22	3.28
1	34	5929.21	4.375	6	31	8588.31	2.672
1	35	6061.84	4.057	6	32	8759.32	1.976
1	36	6195.01	3.707	6	33	8926.92	1.261
1	37	6331.99	3.329	6	34	9092.08	0.589
1	38	6465.35	2.935	6	35	9257.99	0.019
1	39	6594.33	2.531	6	36	9423.84	0.403
1	40	6728.29	2.126	6	37	9598	0.642
2	4	1379.5	0.126	6	38	9760.62	0.667
2	5	1515.22	0.138	6	39	9928.85	0.46
2	6	1681.13	0.108	7	5	3657.53	1.792
2	7	1865.17	0.032	7	6	3955.62	1.743
2	8	2049.48	0.081	7	7	4234.37	1.644
2	9	2228.67	0.056	7	8	4449.41	1.548
2	10	2403.2	0.024	7	9	4614.44	1.469
2	11	2572.35	0.152	7	10	4763.5	1.382
2	12	2737.26	0.321	7	11	4915.5	1.243
2	13	2899.89	0.506	7	12	5069.25	1.01
2	14	3062.36	0.534	7	17	6610.15	4.887
2	27	5746.14	0.21	7	19	6919.81	4.997
2	28	5903.83	0.154	7	20	7077.02	4.683
2	29	6068.16	0.102	7	21	7248.37	4.011
2	30	6228.58	0.046	7	22	7418.74	2.965
2	31	6385.18	0.022	7	23	7593.93	1.64
2	32	6541.11	0.106	7	24	7778.89	0.208
2	33	6697.21	0.21	7	25	7962.79	1.153
2	34	6852.1	0.338	7	26	8154.35	2.325

Continued on next page.

Table S2 – *Continued from previous page.*

n	l	Center frequency (μ Hz)	1σ (μ Hz)	n	l	Center frequency (μ Hz)	1σ (μ Hz)
2	35	7011.93	0.494	7	27	8342.33	3.259
2	36	7164.43	0.681	7	28	8521.34	3.945
2	37	7318.57	0.898	7	29	8709.31	4.403
2	38	7473.02	1.15	7	30	8902.55	4.652
2	39	7623.41	1.432	7	31	9089.32	4.72
2	40	7774.96	1.746	7	32	9279.18	4.631
2	41	7921.26	2.087	7	33	9457.48	4.407
2	42	8069.9	2.452	7	34	9636.85	4.066
2	43	8219.56	2.835	7	35	9820.31	3.632
2	44	8360.56	3.23	8	6	4430.29	0.958
2	45	8508.98	3.631	8	7	4646.44	0.658
2	46	8657.04	4.029	8	10	5503.02	1.815
2	47	8807.29	4.416	8	11	5709.54	1.265
3	6	2548.8	1.489	8	21	7976.33	6.275
3	7	2685.77	1.507	8	22	8127.86	6.066
3	8	2819.24	1.54	9	6	4618.87	2.113
3	9	2951.37	1.569	9	8	5138.46	1.628
3	10	3082.1	1.581	9	10	5606.08	3.779
3	11	3219.5	1.565	9	11	5882.36	1.022
3	12	3361.34	1.519	9	12	6183.67	0.341
3	13	3507.53	1.445	9	13	6480.69	0.77
3	14	3656.18	1.349	9	14	6764.72	0.532
3	15	3810.96	1.237	9	15	7025.3	0.917
3	16	3966.83	1.118	9	16	7232.73	3.614
3	17	4124	0.997	9	18	7541.47	5.71
3	18	4283.79	0.878	10	10	6186.46	3.796
3	19	4446.12	0.766	10	11	6446.65	3.225
3	20	4608.97	0.662	10	12	6684.99	3.063
3	21	4771.58	0.567	10	13	6863.78	3.155
3	22	4932.87	0.487	10	15	7198	2.403
3	23	5098.42	0.419	10	16	7420.13	0.764
3	24	5262.95	0.375	10	17	7672.67	0.792
3	41	8823.12	13.45	10	18	7936.4	2.129
3	42	8976.89	14.382	10	19	8196.77	4.498
3	43	9138.26	15.229	10	20	8446.07	8.138
3	44	9290.13	15.98	10	21	8671.34	12.39
3	45	9442.23	16.627	10	22	8864.68	13.948
3	46	9603.46	17.165	11	9	6431.87	1.645

Continued on next page.

Table S2 – *Continued from previous page.*

n	l	Center frequency (μ Hz)	1σ (μ Hz)	n	l	Center frequency (μ Hz)	1σ (μ Hz)
3	47	9750.65	17.589	11	10	6705.57	1.034
3	48	9908.13	17.895	11	11	6915	1.005
4	1	1411.79	1.297	11	12	7142.96	1.939
4	2	1721.4	1.278	11	13	7411.49	2.515
4	3	2048.27	1.395	11	14	7679.54	3.086
4	4	2278.3	1.495	11	17	8265	3.765
4	5	2411.12	1.486	11	20	8724.19	1.938
4	10	3864.07	2.114	11	21	8896.97	5.558
4	11	4007.5	1.904	11	22	9103.07	6.432
4	12	4151.99	1.714	11	23	9332.87	4.284
4	13	4292.04	1.516	11	24	9570.49	1.475
4	14	4435.29	1.305	11	25	9808.53	1.267
4	15	4583.99	1.086	12	6	5643.85	5.706
4	16	4729.84	0.862	12	7	5852.44	1.645
4	17	4885.31	0.647	12	11	7133.44	0.318
4	18	5043.65	0.447	12	12	7448.91	0.533
4	19	5200.62	0.271	12	13	7769.84	0.115
4	20	5362.18	0.128	12	14	8090.28	0.918
4	21	5526.06	0.028	12	15	8404.52	4.195
4	22	5694.99	0.021	12	16	8686.69	10.085
4	23	5861.47	0.01	12	17	8928.22	9.561
4	24	6028.66	0.071	13	15	8472.66	1.321
4	25	6197.22	0.23	13	16	8744.85	3.228
4	26	6365.48	0.476	13	17	9053.82	1.481
4	27	6535.53	0.815	13	18	9363.72	0.205
4	28	6702.64	1.253	13	19	9664.49	0.874
4	29	6872.94	1.791	13	20	9954.48	1.593
4	30	7038.1	2.431	14	8	7042.53	0.994
4	31	7204.4	3.171	14	9	7344.52	1.933
4	32	7369.38	4.005	14	13	8729.82	9.31
4	33	7536.5	4.923	14	14	8981.49	10.107
4	34	7700.07	5.916	15	12	8427.73	7.664
4	35	7859.57	6.968	15	15	9592.15	2.328
4	36	8019.94	8.06	15	16	9921.12	3.751
4	37	8184.37	9.175	16	10	8433.36	0.99
4	38	8342.14	10.291	16	11	8730.13	1.451
4	39	8499.51	11.388	16	14	9299.32	0.528
4	40	8663.48	12.424	17	12	9148.44	7.792

Continued on next page.

Table S2 – *Continued from previous page.*

n	l	Center frequency (μ Hz)	1σ (μ Hz)	n	l	Center frequency (μ Hz)	1σ (μ Hz)
5	3	2168.68	1.571	17	13	9428.47	4.947
5	4	2379.18	1.633	17	14	9698.54	2.925
5	5	2703.4	1.889	17	15	9932.67	0.558
5	6	3011.05	2.206	19	11	9644.79	3.53
5	7	3291.65	2.566	6	8	3737.51	0.032
5	8	3525.93	2.702	9	9	5381.54	2.705
5	11	4456.88	0.638	10	8	5735	5.169
5	12	4695.77	0.668	10	9	5938.99	4.693
5	13	4925.5	0.778	12	10	6859.99	1.223
5	14	5134.96	1.063	15	11	8122.41	7.67
5	15	5326.87	1.487	18	9	8735	8.06
5	16	5502.45	1.918				

9 Model values

Here we present models of the velocity and density in the outer core as a function of depth for the EPOC-Vinet and EPOC-BM models (tables S3 and S4 respectively). $Q_\kappa = 57823$ is used for the outer core for both EPOC-Vinet and EPOC-BM.

Table S3: The EPOC-Vinet model and associated velocity and density ranges.

Depth (km)	Velocity (kms^{-1})	Density (gcm^{-3})	Velocity 66% interval (kms^{-1})	Density 66% interval (gcm^{-3})
2891.00	7.999	9.996	7.989 – 8.007	9.958 – 10.036
2914.05	8.040	10.035	8.031 – 8.048	9.997 – 10.075
2937.09	8.081	10.073	8.072 – 8.089	10.035 – 10.114
2960.14	8.121	10.111	8.113 – 8.129	10.072 – 10.152
2983.18	8.161	10.149	8.153 – 8.169	10.109 – 10.190
3006.23	8.201	10.186	8.193 – 8.208	10.146 – 10.227
3029.28	8.239	10.222	8.232 – 8.246	10.182 – 10.264
3052.32	8.278	10.258	8.271 – 8.284	10.218 – 10.301
3075.37	8.316	10.294	8.309 – 8.322	10.254 – 10.337
3098.41	8.353	10.330	8.347 – 8.359	10.289 – 10.372
3121.46	8.390	10.365	8.384 – 8.395	10.324 – 10.408
3144.51	8.427	10.399	8.421 – 8.432	10.358 – 10.443
3167.55	8.463	10.434	8.457 – 8.467	10.392 – 10.477

Continued on next page

Table S3 – *Continued from previous page*

Depth (km)	Velocity (kms^{-1})	Density (gcm^{-3})	Velocity 66% interval (kms^{-1})	Density 66% interval (gcm^{-3})
3190.60	8.498	10.468	8.493 – 8.503	10.426 – 10.512
3213.64	8.533	10.501	8.529 – 8.538	10.459 – 10.546
3236.69	8.568	10.535	8.564 – 8.572	10.492 – 10.579
3259.73	8.602	10.568	8.598 – 8.606	10.525 – 10.612
3282.78	8.636	10.600	8.632 – 8.640	10.557 – 10.645
3305.83	8.670	10.632	8.666 – 8.673	10.589 – 10.678
3328.87	8.703	10.664	8.700 – 8.706	10.621 – 10.710
3351.92	8.736	10.696	8.732 – 8.738	10.652 – 10.742
3374.96	8.768	10.727	8.765 – 8.770	10.683 – 10.773
3398.01	8.800	10.758	8.797 – 8.802	10.714 – 10.804
3421.06	8.831	10.788	8.829 – 8.834	10.744 – 10.835
3444.10	8.863	10.819	8.860 – 8.865	10.774 – 10.866
3467.15	8.893	10.849	8.891 – 8.895	10.804 – 10.896
3490.19	8.924	10.878	8.921 – 8.926	10.833 – 10.926
3513.24	8.954	10.907	8.952 – 8.956	10.862 – 10.955
3536.29	8.984	10.936	8.981 – 8.985	10.891 – 10.984
3559.33	9.013	10.965	9.011 – 9.015	10.919 – 11.013
3582.38	9.042	10.994	9.039 – 9.044	10.947 – 11.042
3605.42	9.070	11.022	9.068 – 9.073	10.975 – 11.070
3628.47	9.099	11.049	9.096 – 9.101	11.003 – 11.098
3651.52	9.127	11.077	9.124 – 9.129	11.030 – 11.126
3674.56	9.154	11.104	9.152 – 9.157	11.057 – 11.153
3697.61	9.182	11.131	9.179 – 9.184	11.084 – 11.181
3720.65	9.209	11.158	9.205 – 9.212	11.110 – 11.208
3743.70	9.235	11.184	9.232 – 9.238	11.136 – 11.234
3766.74	9.262	11.210	9.258 – 9.265	11.162 – 11.260
3789.79	9.288	11.236	9.284 – 9.291	11.188 – 11.286
3812.84	9.313	11.261	9.309 – 9.317	11.213 – 11.312
3835.88	9.339	11.287	9.335 – 9.343	11.238 – 11.338
3858.93	9.364	11.312	9.360 – 9.368	11.263 – 11.363
3881.97	9.389	11.336	9.384 – 9.393	11.287 – 11.388
3905.02	9.413	11.361	9.408 – 9.418	11.312 – 11.412
3928.07	9.437	11.385	9.432 – 9.442	11.336 – 11.437
3951.11	9.461	11.409	9.456 – 9.466	11.359 – 11.461
3974.16	9.485	11.432	9.480 – 9.490	11.383 – 11.485
3997.20	9.508	11.456	9.503 – 9.513	11.406 – 11.508
4020.25	9.531	11.479	9.525 – 9.537	11.429 – 11.531

Continued on next page

Table S3 – *Continued from previous page*

Depth (km)	Velocity (kms^{-1})	Density (gcm^{-3})	Velocity 66% interval (kms^{-1})	Density 66% interval (gcm^{-3})
4043.30	9.554	11.502	9.548 – 9.560	11.451 – 11.554
4066.34	9.576	11.524	9.570 – 9.582	11.474 – 11.577
4089.39	9.599	11.547	9.592 – 9.605	11.496 – 11.600
4112.43	9.620	11.569	9.614 – 9.627	11.518 – 11.622
4135.48	9.642	11.590	9.635 – 9.649	11.539 – 11.644
4158.53	9.663	11.612	9.657 – 9.670	11.561 – 11.666
4181.57	9.685	11.633	9.678 – 9.691	11.582 – 11.687
4204.62	9.705	11.654	9.698 – 9.712	11.603 – 11.708
4227.66	9.726	11.675	9.719 – 9.733	11.624 – 11.729
4250.71	9.746	11.696	9.739 – 9.754	11.644 – 11.750
4273.76	9.766	11.716	9.758 – 9.774	11.664 – 11.771
4296.80	9.786	11.736	9.778 – 9.794	11.684 – 11.791
4319.85	9.805	11.756	9.797 – 9.813	11.704 – 11.811
4342.89	9.825	11.776	9.816 – 9.833	11.723 – 11.831
4365.94	9.844	11.795	9.835 – 9.852	11.742 – 11.850
4388.98	9.862	11.814	9.854 – 9.871	11.761 – 11.869
4412.03	9.881	11.833	9.872 – 9.890	11.780 – 11.888
4435.08	9.899	11.851	9.890 – 9.908	11.799 – 11.907
4458.12	9.917	11.870	9.908 – 9.926	11.817 – 11.926
4481.17	9.935	11.888	9.926 – 9.944	11.835 – 11.944
4504.21	9.952	11.906	9.943 – 9.962	11.853 – 11.962
4527.26	9.970	11.924	9.960 – 9.979	11.870 – 11.980
4550.31	9.987	11.941	9.977 – 9.996	11.887 – 11.998
4573.35	10.003	11.958	9.994 – 10.013	11.905 – 12.015
4596.40	10.020	11.975	10.010 – 10.030	11.921 – 12.032
4619.44	10.036	11.992	10.026 – 10.046	11.938 – 12.049
4642.49	10.052	12.009	10.042 – 10.063	11.954 – 12.066
4665.54	10.068	12.025	10.058 – 10.079	11.971 – 12.082
4688.58	10.084	12.041	10.073 – 10.094	11.987 – 12.098
4711.63	10.099	12.057	10.089 – 10.110	12.002 – 12.114
4734.67	10.114	12.072	10.104 – 10.125	12.018 – 12.130
4757.72	10.129	12.088	10.118 – 10.140	12.033 – 12.145
4780.77	10.144	12.103	10.133 – 10.155	12.048 – 12.161
4803.81	10.158	12.118	10.147 – 10.170	12.063 – 12.176
4826.86	10.173	12.133	10.161 – 10.184	12.078 – 12.191
4849.90	10.187	12.147	10.175 – 10.198	12.092 – 12.205
4872.95	10.201	12.162	10.189 – 10.212	12.106 – 12.220

Continued on next page

Table S3 – *Continued from previous page*

Depth (km)	Velocity (kms^{-1})	Density (gcm^{-3})	Velocity 66% interval (kms^{-1})	Density 66% interval (gcm^{-3})
4895.99	10.214	12.176	10.202 – 10.226	12.120 – 12.234
4919.04	10.227	12.190	10.216 – 10.239	12.134 – 12.248
4942.09	10.241	12.203	10.229 – 10.252	12.148 – 12.262
4965.13	10.254	12.217	10.241 – 10.266	12.161 – 12.275
4988.18	10.266	12.230	10.254 – 10.278	12.174 – 12.288
5011.22	10.279	12.243	10.266 – 10.291	12.187 – 12.302
5034.27	10.291	12.256	10.279 – 10.303	12.200 – 12.314
5057.32	10.303	12.268	10.291 – 10.316	12.212 – 12.327
5080.36	10.315	12.281	10.302 – 10.328	12.225 – 12.340
5103.41	10.327	12.293	10.314 – 10.339	12.237 – 12.352
5126.45	10.338	12.305	10.325 – 10.351	12.249 – 12.364
5149.50	10.349	12.317	10.336 – 10.362	12.260 – 12.376

Table S4: The EPOC-BM model and associated velocity and density ranges.

Depth (km)	Velocity (kms^{-1})	Density (gcm^{-3})	Velocity 66% interval (kms^{-1})	Density 66% interval (gcm^{-3})
2891.00	8.014	9.997	8.005 – 8.024	9.958 – 10.035
2914.05	8.054	10.035	8.045 – 8.063	9.996 – 10.074
2937.09	8.093	10.074	8.085 – 8.102	10.034 – 10.113
2960.14	8.132	10.111	8.124 – 8.141	10.071 – 10.151
2983.18	8.171	10.149	8.163 – 8.179	10.108 – 10.188
3006.23	8.209	10.186	8.202 – 8.217	10.145 – 10.226
3029.28	8.247	10.222	8.240 – 8.254	10.181 – 10.262
3052.32	8.284	10.258	8.277 – 8.291	10.217 – 10.299
3075.37	8.321	10.294	8.314 – 8.327	10.253 – 10.335
3098.41	8.357	10.330	8.351 – 8.363	10.288 – 10.371
3121.46	8.393	10.365	8.388 – 8.399	10.322 – 10.406
3144.51	8.429	10.399	8.423 – 8.434	10.357 – 10.441
3167.55	8.464	10.434	8.459 – 8.469	10.391 – 10.475
3190.60	8.499	10.467	8.494 – 8.504	10.425 – 10.510
3213.64	8.533	10.501	8.529 – 8.538	10.458 – 10.544
3236.69	8.567	10.534	8.563 – 8.572	10.491 – 10.577
3259.73	8.601	10.567	8.597 – 8.605	10.524 – 10.610
3282.78	8.634	10.600	8.631 – 8.638	10.556 – 10.643
3305.83	8.667	10.632	8.664 – 8.671	10.588 – 10.676
3328.87	8.700	10.664	8.697 – 8.703	10.619 – 10.708
3351.92	8.732	10.696	8.730 – 8.735	10.651 – 10.740
3374.96	8.764	10.727	8.762 – 8.767	10.682 – 10.771
3398.01	8.796	10.758	8.794 – 8.799	10.712 – 10.802
3421.06	8.827	10.788	8.825 – 8.830	10.743 – 10.833
3444.10	8.858	10.819	8.856 – 8.861	10.773 – 10.864
3467.15	8.889	10.849	8.887 – 8.891	10.802 – 10.894
3490.19	8.919	10.878	8.917 – 8.921	10.832 – 10.924
3513.24	8.949	10.907	8.947 – 8.951	10.861 – 10.953
3536.29	8.978	10.937	8.977 – 8.981	10.890 – 10.983
3559.33	9.008	10.965	9.006 – 9.010	10.918 – 11.012
3582.38	9.037	10.994	9.035 – 9.039	10.946 – 11.040
3605.42	9.065	11.022	9.063 – 9.068	10.974 – 11.069
3628.47	9.094	11.050	9.091 – 9.096	11.002 – 11.097
3651.52	9.122	11.077	9.119 – 9.124	11.029 – 11.124
3674.56	9.149	11.104	9.147 – 9.152	11.056 – 11.152
3697.61	9.177	11.131	9.174 – 9.180	11.083 – 11.179

Continued on next page

Table S4 – *Continued from previous page*

Depth (km)	Velocity (kms^{-1})	Density (gcm^{-3})	Velocity 66% interval (kms^{-1})	Density 66% interval (gcm^{-3})
3720.65	9.204	11.158	9.201 – 9.207	11.109 – 11.206
3743.70	9.231	11.184	9.228 – 9.234	11.136 – 11.233
3766.74	9.257	11.211	9.254 – 9.261	11.161 – 11.259
3789.79	9.284	11.236	9.280 – 9.287	11.187 – 11.285
3812.84	9.309	11.262	9.306 – 9.314	11.212 – 11.311
3835.88	9.335	11.287	9.331 – 9.339	11.237 – 11.336
3858.93	9.360	11.312	9.356 – 9.365	11.262 – 11.361
3881.97	9.386	11.337	9.381 – 9.390	11.287 – 11.386
3905.02	9.410	11.361	9.406 – 9.415	11.311 – 11.411
3928.07	9.435	11.385	9.430 – 9.440	11.335 – 11.435
3951.11	9.459	11.409	9.454 – 9.464	11.359 – 11.459
3974.16	9.483	11.433	9.478 – 9.488	11.382 – 11.483
3997.20	9.507	11.456	9.501 – 9.512	11.405 – 11.507
4020.25	9.530	11.479	9.525 – 9.536	11.428 – 11.530
4043.30	9.553	11.502	9.548 – 9.559	11.451 – 11.553
4066.34	9.576	11.525	9.570 – 9.582	11.473 – 11.576
4089.39	9.599	11.547	9.593 – 9.605	11.495 – 11.598
4112.43	9.621	11.569	9.615 – 9.628	11.517 – 11.620
4135.48	9.643	11.591	9.637 – 9.650	11.539 – 11.642
4158.53	9.665	11.613	9.658 – 9.672	11.560 – 11.664
4181.57	9.686	11.634	9.680 – 9.694	11.581 – 11.685
4204.62	9.708	11.655	9.701 – 9.715	11.602 – 11.707
4227.66	9.729	11.676	9.722 – 9.736	11.623 – 11.728
4250.71	9.750	11.696	9.742 – 9.757	11.643 – 11.748
4273.76	9.770	11.717	9.763 – 9.778	11.663 – 11.769
4296.80	9.790	11.737	9.783 – 9.798	11.683 – 11.789
4319.85	9.810	11.756	9.802 – 9.819	11.703 – 11.809
4342.89	9.830	11.776	9.822 – 9.838	11.722 – 11.829
4365.94	9.850	11.795	9.841 – 9.858	11.741 – 11.848
4388.98	9.869	11.814	9.861 – 9.878	11.760 – 11.867
4412.03	9.888	11.833	9.879 – 9.897	11.779 – 11.886
4435.08	9.907	11.852	9.898 – 9.916	11.797 – 11.905
4458.12	9.925	11.870	9.916 – 9.934	11.816 – 11.924
4481.17	9.943	11.888	9.935 – 9.953	11.834 – 11.942
4504.21	9.962	11.906	9.952 – 9.971	11.851 – 11.960
4527.26	9.979	11.924	9.970 – 9.989	11.869 – 11.978
4550.31	9.997	11.941	9.987 – 10.007	11.886 – 11.995

Continued on next page

Table S4 – *Continued from previous page*

Depth (km)	Velocity (kms^{-1})	Density (gcm^{-3})	Velocity 66% interval (kms^{-1})	Density 66% interval (gcm^{-3})
4573.35	10.014	11.958	10.005 – 10.024	11.903 – 12.013
4596.40	10.031	11.975	10.022 – 10.041	11.920 – 12.030
4619.44	10.048	11.992	10.038 – 10.058	11.937 – 12.047
4642.49	10.065	12.009	10.055 – 10.075	11.953 – 12.063
4665.54	10.081	12.025	10.071 – 10.092	11.969 – 12.080
4688.58	10.097	12.041	10.087 – 10.108	11.985 – 12.096
4711.63	10.113	12.057	10.103 – 10.124	12.001 – 12.112
4734.67	10.129	12.072	10.118 – 10.140	12.016 – 12.127
4757.72	10.144	12.088	10.134 – 10.155	12.032 – 12.143
4780.77	10.160	12.103	10.149 – 10.171	12.047 – 12.158
4803.81	10.175	12.118	10.164 – 10.186	12.061 – 12.173
4826.86	10.190	12.132	10.178 – 10.201	12.076 – 12.188
4849.90	10.204	12.147	10.193 – 10.216	12.090 – 12.203
4872.95	10.218	12.161	10.207 – 10.230	12.105 – 12.217
4895.99	10.233	12.175	10.221 – 10.244	12.118 – 12.231
4919.04	10.246	12.189	10.235 – 10.258	12.132 – 12.245
4942.09	10.260	12.203	10.249 – 10.272	12.146 – 12.259
4965.13	10.274	12.216	10.262 – 10.286	12.159 – 12.272
4988.18	10.287	12.229	10.275 – 10.299	12.172 – 12.285
5011.22	10.300	12.242	10.288 – 10.312	12.185 – 12.298
5034.27	10.313	12.255	10.301 – 10.325	12.198 – 12.311
5057.32	10.325	12.268	10.313 – 10.338	12.210 – 12.324
5080.36	10.338	12.280	10.325 – 10.350	12.222 – 12.336
5103.41	10.350	12.292	10.337 – 10.363	12.234 – 12.348
5126.45	10.362	12.304	10.349 – 10.375	12.246 – 12.360
5149.50	10.374	12.316	10.361 – 10.387	12.258 – 12.372